Ecological Indicators 189 (2026) 115235

Contents lists available at ScienceDirect

Ecological Indicators

journal homepage: www.elsevier.com/locate/ecolind

A remote sensing-based tree mortality indicator for biodiversity monitoring using multispectral UAV and lidar in the Arctic region, Finland

Katalin Waga [a,*], Jaan Rönkkö [b], Mikko Kukkonen [c], Anton Kuzmin [d], Timo Kumpula [d], Parvez Rana [b]

[a] LUKE Natural Resources Institute Finland, Ounasjoentie 6, 96200 Rovaniemi, Finland
[b] LUKE Natural Resources Institute Finland, Latokartanonkaari 9, 00790 Helsinki, Finland
[c] LUKE Natural Resources Institute Finland, Paavo Havaksen tie 3, 90570 Oulu, Finland
[d] Department of Geographical and Historical Studies, University of Eastern Finland, Finland

ARTICLE INFO

Keywords:
Ecological indicator
Tree mortality
Biodiversity monitoring
Deadwood
Deep learning
U-net
Image segmentation
Remote sensing
UAV multispectral imagery

ABSTRACT

Deadwood is a recognised ecological indicator for forest biodiversity. Both the UN Convention on Biological Diversity and the EU Biodiversity Strategy 2030 mandates inventorying and reporting deadwood. However, monitoring tree mortality, the source of deadwood, remains challenging, especially in Arctic and sub-Arctic regions. Boreal forests in this region face increasing climate-driven stressors: droughts, pest outbreaks, and snow damage. These stressors accelerate tree mortality and threaten biodiversity. Deep learning-based semantic segmentation offers a scalable solution for monitoring standing tree mortality using remote sensing data such as multispectral UAV imagery and lidar-derived canopy height models. In this study, we (1) evaluated a U-Net model for detecting tree mortality across 208 ha of *Picea abies*, *Pinus sylvestris*, and deciduous dominated forests, and (2) produced a wall-to-wall mortality map to identify spatial patterns and potential drivers in Northern Lapland, Finland. The training dataset included 411 tiles containing 4380 manually delineated tree crowns. The model achieved an overall accuracy of 0.92, with a recall and F1-score for dead trees 0.82 and 0.57, for alive trees 0.93 and 0.96. The performance is sufficient for identifying spatial patterns despite false positive detections. Mortality hotspots were concentrated in *Picea abies* dominated areas at higher elevations where older trees were located, suggesting a link to snow damage besides natural mortality. These results demonstrate the potential of UAV based deep learning workflows for large-scale exploratory monitoring of tree mortality patterns in northern boreal forests in Arctic and sub-Arctic region and supports biodiversity reporting and restoration monitoring through spatial forest-health assessment.

1. Introduction

1.1. Tree mortality indicator for biodiversity monitoring

Dead trees play a crucial indicator role in understanding and managing forest ecosystems, especially in the context of climate resilience, forest health, and biodiversity conservation. Due to climate change, forests face increasing stress from droughts, pest outbreaks, and changing snow cover patterns, particularly in the Arctic and sub-Arctic regions (Liu et al., 2024; Mudryk et al., 2024; Singh et al., 2024).

Trees die as a result of natural mortality and various biotic and abiotic stressors. Bark beetle infestations devastated coniferous forests across Europe and North America (Francis et al., 2025), but other pathogens, such as *Phytophthora* species (e.g., *Phytophthora cinnamomi*, *P. ramorum*), *Armillaria* root rot (e.g., *Armillaria mellea*) (U.S. Forest Service, 2024), or pinewood nematode (Han et al., 2022), attack and kill trees with quick pace too. Climate-induced droughts reduce tree vitality and increase susceptibility to pests and diseases (Biedermann et al., 2019; Junttila et al., 2024; Robbins et al., 2021). Arctic and sub-Arctic forest ecosystems are particularly sensitive to climate change because they are characterized by short growing seasons, low temperature margins, and slow ecosystem recovery rates (Christiani et al., 2025). Even relatively small increases in temperature or changes in snow cover can therefore result in disproportionately large impacts on tree growth, stability, and mortality (Lehtonen et al., 2014; Martz et al., 2016; Nykänen et al., 1997). Recent warming in the Arctic has exceeded

* Corresponding author.
E-mail address: katalin.waga@luke.fi (K. Waga).

https://doi.org/10.1016/j.ecolind.2026.115235
Received 31 March 2026; Received in revised form 19 June 2026; Accepted 16 July 2026
Available online 24 July 2026

the global average due to Arctic amplification (Rantanen et al., 2022) leading shifts in snow load dynamics, increased freeze–thaw cycles, and soil moisture conditions, all of which directly affect tree survival (Kosolapova and Altshuler, 2024). Snow cover dynamics of these regions characterized with fluctuating snow loads can damage both tree crowns and stems and can lead to increased insect attacks (Lehtonen et al., 2014; Nykänen et al., 1997). International conventions, not limited to the United Nation's Convention on Biological Diversity (United Nations, 1992) and Forest Europe, former Ministerial Conference on the Protection of Forests in Europe (Forest Europe, former M. C. on the P. of F. in E., 2020), also emphasize the ecological value of dead wood as a key indicator for biodiversity and sustainable forest management. Boreal forests in Arctic and sub-Arctic region have a crucial role in regulating the long-term climate change effects in every prediction scenario prepared by UN (United Nations, 2023). EU Biodiversity Strategy 2030 also requires that member states report tree mortality as a part of Nature Restoration Regulation (NRR), where standing and lying deadwood are the first two indicators for forest restoration monitoring (European commission, 2024). Indicators such as deadwood simplify complex ecological processes into measurable attributes, enabling standardized monitoring across different regions, and supporting international biodiversity targets (Chapin et al., 2010; Slepetiene et al., 2025).

Deadwood is widely recognised as a biodiversity indicator due to its presence and diversity correlate strongly with species richness, particularly saproxylic organisms such as fungi, beetles and cavity-nesting birds (Lassauce et al., 2011; Parajuli and Markwith, 2023). Deadwood occurs naturally through tree senescence, but is also generated by tree mortality caused by disturbances. Forest management practices, including timber harvesting, clearcutting, and fire suppression, substantially reduce the amount of deadwood. Climate change is further expected to alter deadwood availability as trees die earlier than they would by natural mortality, therefore their individual sizes are smaller. Natural mortality refers to tree death caused by senescence and non-anthropogenic disturbances. In boreal forest of the Arctic and sub-Arctic region of Finland, coniferous deadwood from Norway spruce (*Picea abies* H. Karst.) and Scots Pine (*Pinus sylvestris* L.) supports a higher number of red-list species than deciduous deadwood (Rana and Tolvanen, 2021; Tikkanen et al., 2006).

The Arctic warmed four times faster (Rantanen et al., 2022) than the global average since 1979. The increased temperature means increased growth that leads to denser stands where trees compete more for water, light, and nutrients (Ford et al., 2017; Way and Oren, 2010). Due to this increased competition, the trees are more vulnerable to stress and mortality. Shorter lifespan means that trees do not grow as old and tall and they die earlier than they would, leaving less amount of deadwood in the forest. Increased growth also leads to larger growth rings that make stems weaker, increasing the risk of snow and wind damage (Kretschmann, 2010; Nykänen et al., 1997).

Another effect of climate change is the more frequent and stronger disturbances whether it is storms with strong winds, drought, or pests' outbreaks. These disturbances increased significantly during the last 70 years (Patacca et al., 2023), and they all cause sudden mortality of trees that were potentially decades away from natural death. The decomposition rate is also more rapid in warmer conditions as the microbial activity speeds up, leading to a more rapid decay process. More frequent and intense forest fires also lessen the wood amount, including the future dead wood amount left in the forest.

The changing conditions (e.g. warmer and drier) also cause shift in tree species composition. *Picea abies* has shallow roots and does not tolerate drought well, moreover, drought increases their susceptibility to bark beetle attacks (Netherer et al., 2024). Even though *Pinus sylvestris* has deeper roots, it is still vulnerable in very dry sites but predicted to benefit from climate change in the Arctic region by longer growth seasons (Martinez del Castillo et al., 2024).The changing conditions favour birches, as they are fast growing and lot more adaptable, therefore they are more often considered as a suitable tree species in climate smart silviculture and mixed species forestry due to their resilience. Other broadleaves such as aspen also a good example that expected to spread more due to their fast regeneration after fire or wind damage and tolerates different moisture and soil conditions well (McIlroy and Shinneman, 2020). Larches also benefit from climate change based on study in northern Siberia (Kharuk et al., 2022) as the growing season extends, and they respond well for changing moisture conditions and tolerates permafrost thaw better then *Picea abies*. Tracking tree mortality patterns under changing conditions provides insights into forest resilience and helps predict effects on carbon storage and habitat availability.

1.2. Dead tree detection using deep learning

Despite its importance, mapping of deadwood remains challenging at larger scales due to field work limitations. Recent development in remote sensing and deep learning offer better detection and measurement possibilities of dead trees. Threshold-based indices, object-based approaches, and classical machine learning models have previously been used to map vegetation condition; however, these methods rely on hand-crafted features, site-specific thresholds, or segmented objects that limit scalability across large areas (Prieur et al., 2022; Rana et al., 2022; Zhang et al., 2021). In contrast, U-Net enables direct multi-class pixel-wise learning that integrates spectral and structural information without manual rule definition.

Uncrewed aerial vehicle (UAV)-based imagery offers several advantages over satellite remote sensing for monitoring tree mortality. The centimeter-level spatial resolution of UAV data enables the identification of individual tree crowns, fine-scale structural damage, and subtle spectral differences between dead and living vegetation that are not detectable with current satellite sensors (Bergmüller and Vanderwel, 2022; Sun et al., 2021). UAV campaigns can also be timed flexibly to optimal phenological conditions, reducing ambiguity caused by seasonal variation. In addition, UAV data provide high-quality reference information that can be used for training and validating models intended for coarser-resolution satellite observations (Keränen et al., 2024). While satellite imagery is indispensable for large-scale and frequent monitoring, UAV-based approaches play a complementary role by enabling detailed mortality detection and calibration of scalable forest health indicators.

Semantic segmentation is an artificial intelligence (AI)-aided deep learning method where every pixel is assigned to a certain class, while instance segmentation identifies certain object on an image (Yasir and Ahn, 2022). Most studies rely on convolutional neural networks (CNNs), with frameworks such as U-Net for pixel-level segmentation (Ronneberger et al., 2015) or YOLO for object detections (Redmon et al., 2016).

Previous studies have applied deep learning for forest health monitoring using both binary and multi-class classification approaches either on tree or pixel-level. Binary classification, which typically distinguishes dead trees from the background vegetation and other non-dead trees, has achieved strong performance across various studies, often reporting F1-score above 0.80 (Hart and Veblen, 2015; Junttila et al., 2024; Schiefer et al., 2023; Sylvain et al., 2019). These deep learning methods commonly use CNN architectures, such as U-Net on multispectral aerial imagery. Multi-class approaches extend the classification to differentiate healthy, infected, and dead trees, or even species-level distinctions (Kanerva et al., 2022; Kuzmin et al., 2026; Puliti et al., 2025), though accuracy tends to decline as class complexity increases. Tree-level methods generally show lower performance than pixel level segmentations, particularly for infected trees, even though these tree-level classifications sometimes discard non-labelled or ambiguous trees if they aren't identified as trees during the application phase too. Recent works also explore object detection models (e.g. YOLOv8, Faster R-CNN) for standing deadwood detections (Mäyrä et al., 2021, 2025) combined with spectral indices for disease detection (Xu et al., 2024). Multi-class segmentation remains less common and often underperforms binary segmentation, with F1-scores ranging from 52 to 71% for damaged or dead tree classes (Gonzalez and Wallner, 2025; Schwarz et al., 2023).

Despite these advances, most studies either focus on binary classification or rely on tree extraction steps, limiting scalability for large-area monitoring. Multi-class segmentation directly on forest imagery without prior delineation is still unexplored and present challenges in distinguishing subtle health states, our study addresses this gap by applying a multi-class segmentation model on high resolution imagery, with a Ground Sampling Distance (GSD) of 5.2 cm, without tree extraction, aiming to improve prediction accuracy and scalability.

1.3. Objectives of the study

In this study, we develop and validate a remote sensing-based tree mortality indicator to support biodiversity monitoring in boreal forests using a U-Net based deep learning model. The indicandum, defined as the spatial intensity of fully dead standing trees, serves as a proxy for deadwood availability, an essential component for biodiversity and forest health. Trees with partial dead crowns or dead branches were intentionally grouped with the alive tree class to ensure indicator robustness, reproducibility, and scalability across large areas. Fallen deadwood was not included in this study because it cannot be reliably detected from UAV optical imagery and sparse lidar data and would require alternative data sources or field-based inventories beyond the scope of this work (Schiefer et al., 2023). The indicator quantifies this indicandum as the percentage of each 16 m $\times$ 16 m grid cell covered by pixels classified as dead standing trees. An area-based approach was selected instead of crown-based metrics, as it better represents sparse tree cover typical of mire environments. In such conditions, crown-based measures would overestimate mortality in grid cells where a single dead tree occurs without surrounding live trees. We integrate multispectral UAV imagery combined with canopy height model (CHM) derived from low-density (0.5 points per square meter) national lidar data as input datasets and apply semantic segmentation for identifying dead tree pixels.

The study has two objectives: (1) assess the U-Net model's performance in dead tree detection in three different tree species dominated forest areas: *Pinus sylvestris*, *Picea abies*, and deciduous dominated areas to determine the model reliability in different forest covered areas; (2) develop a scalable indicator to identify mortality hotspots. We create a scalable dead tree detection U-Net model for boreal forests in Arctic region and produce a wall-to-wall tree mortality map across the Välisuo study area in Northern Lapland, Finland. Finally, we identified key environmental drivers that contribute to tree mortality and affect forest health in the study area. Our approach enables larger scale, landscape-level monitoring and providing an automated indicator for biodiversity monitoring and forest health.

2. Materials and methods

2.1. Study area

The Välisuo study area is located in Northern Lapland, Finland, near Lake Pallasjärvi in boreal forest zone's Arctic region (Fig. 1). The study area covers 208 ha and lies at elevation ranging between 281 and 375 m above sea level. The Pallas-Yllästunturi fell region characterized by fells with sloped terrain, coniferous forests and scattered mires. The mean monthly temperature ranges between −12.7 °C and + 15.6 °C (Finnish Meteorological Institute, 2025) and the annual precipitation is 500–700 mm, which during the winter months falls in the form of snow. The growing season is short, between 90 and 120 days, and the snow cover last for 6 to 7 months.

The vegetation of the study area is dominated by boreal coniferous forests. About two third of the forest area is covered by *Picea abies* dominant and one third by *Pinus sylvestris* dominant forests. The main tree species are *Picea abies*, *Pinus sylvestris*, Silver Birch (*Betula pendula* Roth), and Downy birch (*Betula pubescens* Ehrh.). There are smaller batches of deciduous dominant forests mainly with these birch species.

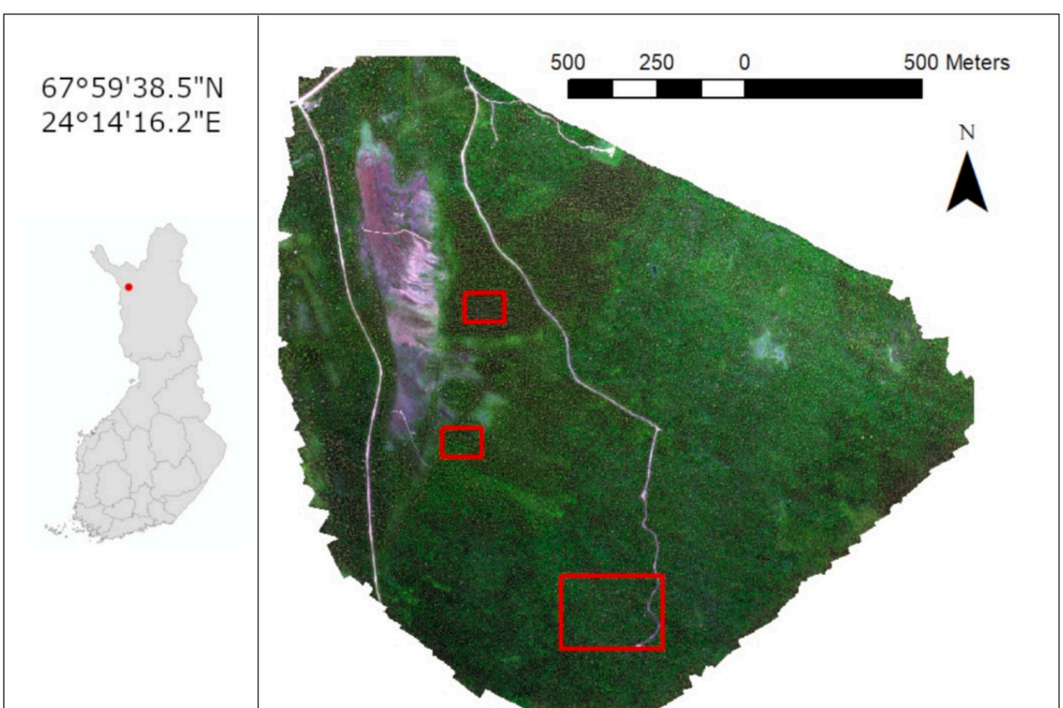

Fig. 1. The location of the Välisuo study area and the three smaller training areas (red rectangles). From the top to bottom, the tree areas are mainly *Pinus sylvestris* dominated, deciduous dominated, and *Picea abies* dominated segments. (For interpretation of the references to colour in this figure legend, the reader is referred to the web version of this article.)

The treeless mire area was drained in the 1960s - 1970s and currently under restoration (Pakalne, 2025). Forests are mostly 50–140 years old, with dominant tree heights ranging from 12.5 to 16 m. The prevailing site type is MT (*Myrtillus* type) (Cajander, 1926), typical of mesic heath forests, and soils are mainly mineral soils with occasional peat patches (Natural Resources Institute Finland, 2016).

2.2. Training area selection and forest inventory data

Forest inventory data provided by the Finnish Forest Center (Suomen Metsäkeskus, 2018) included stand-level attributes such as tree species, dominant height, mean age, and fertility class. Three training areas were selected to represent the species composition, age structure, and dominant height distribution of the entire 206 ha Välisuo site (Figs. 2 and 3) analysing these stand-level attributes of data acquired from the Finnish Forest Centre. The selection criteria included assessing the following parameters in 16 m × 16 m grids: ensuring the representation of *Picea abies*, *Pinus sylvestris*, and deciduous dominated stands, covering representatively all age classes from young mature to old stands, and height variation of the trees. Age classes refer to stand development stages defined in forest inventory data provided by the Finnish Forest Centre, representing broad categories of forest age (e.g. young, mature, and regeneration-ready stands) assigned at the stand or grid level rather than to individual trees. Together these three areas provide a balanced and representative sample for modelling and analysis, ensuring that the trained model reflects the ecological and structural diversity of the Välisuo landscape rather than being biased toward a specific forest type.

2.3. Multispectral imagery and lidar point cloud data

The Välisuo multispectral dataset was acquired on 22 July 2023 using the MicaSense Altum-PT Sensor mounted on a DJI Matrice 300 RTK. Altum multispectral sensor captures images in 5 spectral bands: blue (475 nm center, 32 nm bandwidth), green (560 nm center, 27 nm bandwidth), red (668 nm center, 14 nm bandwidth), red edge (717 nm center, 12 nm bandwidth), and near-infrared (NIR) (842 nm center, 57 nm bandwidth). Images captured for this study cover approximately 208 ha in total. To ensure radiometric stability, the MicaSense Altum-PT was operated with its integrated downwelling light sensor to account for changing illumination during acquisition. Radiometric reference panels with known reflectance properties were captured immediately before and after each flight to support post-processing calibration. The survey was conducted at an altitude of 120 m above ground level, with 85% forward and 75% side image overlap, resulting a ground sampling distance of approximately 5 cm. Positioning and trajectory corrections were obtained in real time through the Finnish VRS network to ensure high geospatial accuracy.

A Canopy Height Model (CHM) derived from low-density (0.5 points/m^2) airborne LiDAR data collected in 2018–2019 from the National Land Survey of Finland (National Land Survey of Finland, 2020). The CHM interpolated using TIN-interpolation and a pit-free algorithm (Khosravipour et al., 2014) and rasterized at the spatial resolution of 1 m.

2.4. Training data preparation

Deep learning methods require extensive training data. We created 4380 tree polygons by visually interpreting multispectral (MS) imagery and manually delineating tree crowns based on the drone images in ArcGIS Desktop 10.8.2 (Fig. 4). The forests were then classified into different classes, fully dead standing trees, alive trees, and background, based on their spectral and structural characteristics on the high-resolution MS bands. During the manual delineation, the following visual cues were used to identify dead trees. On false-colour composites of NIR-red-green, healthy vegetation appears bright red tones due to strong NIR reflectance whereas dead trees appear as greenish hues. This green colour is caused by the loss of NIR reflectance combined with relative higher reflectance in the visible green band. On red edge composites (red-edge-red-green), dead trees frequently appear blue, reflecting their lower reflectance in red-edge and NIR compared to alive trees. We also looked for texture and structure cues: dead trees show more visible branch structure, reduced canopy density, and generally desaturated appearance in visible bands. These tree polygons were then rasterized with the same spatial resolution as the MS imagery. The tree mask polygons included three classes: alive trees, dead trees, and background (everything else which is not a standing tree).

The five MS bands were stacked with the CHM into a 6-band composite used as input for model training. Then overlapping data tiles of the size of 256 × 256 pixels were extracted from both the tree masks and the MS imagery. The training data was created using R 4.5.2 in RStudio 2025.9.2. In total 411 tiles were created both from masks and MS imagery with the edge length of 13.3 m. Data augmentation techniques were applied during training to improve model generalization and increase training data. These included horizontal and vertical flipping and rotation. Additionally, tiles containing more than 5% missing values (NaN) in either imagery or the mask, were discarded to ensure data quality. NaN filtering removed tiles from the edge of the area where missing data occurred.

2.5. U-Net model for tree mortality detection

We implemented a U-Net model (Ronneberger et al., 2015) which is well-suited for semantic segmentation tasks in remote sensing. Semantic segmentation is suitable for indicator quantification, as pixel-level

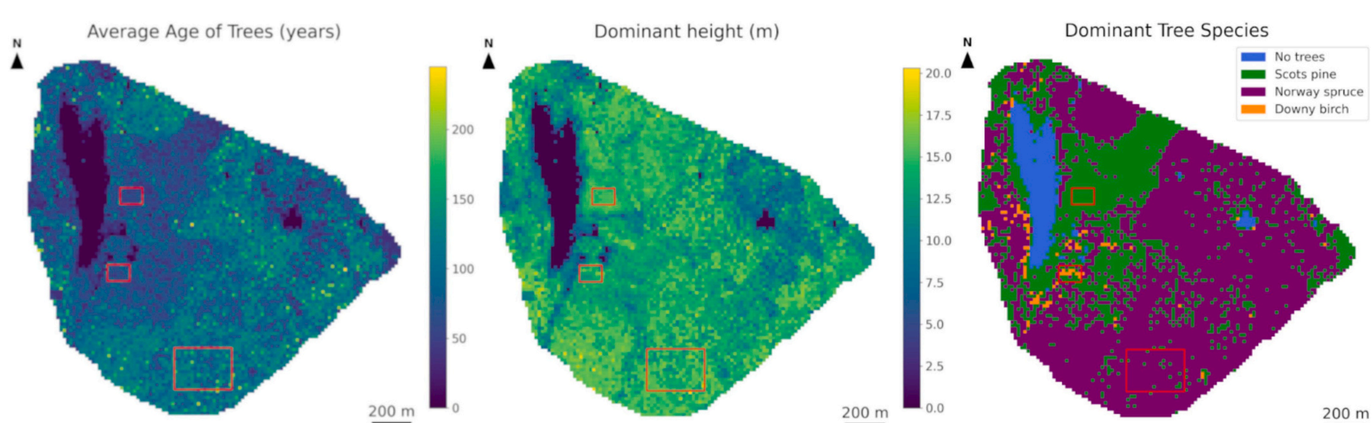

Fig. 2. The average age of trees (year), dominant height (m) and dominant tree species in Välisuo area. The red rectangles mark the areas used for training the model. (For interpretation of the references to colour in this figure legend, the reader is referred to the web version of this article.)

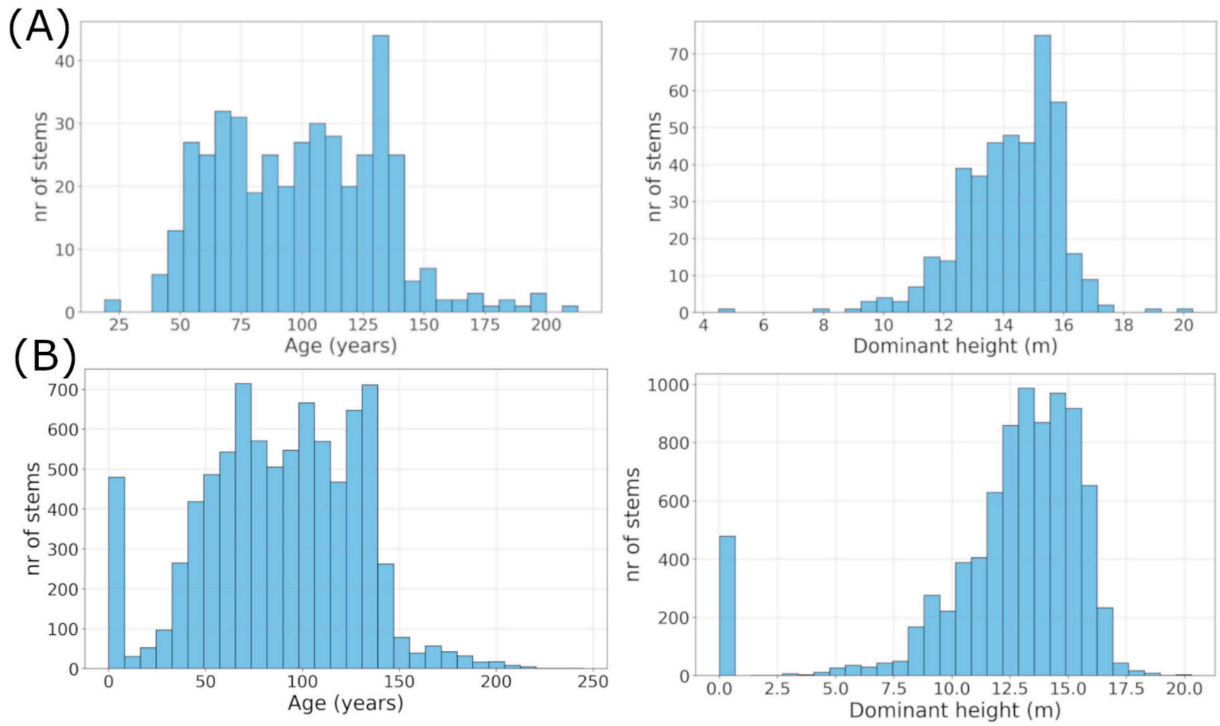

Fig. 3. Age and dominant height distribution of trees at stand-level in the training area (A) and the whole Välisuo area (B) based on the data acquired from the Finnish Forest Center (Suomen Metsäkeskus, 2018).

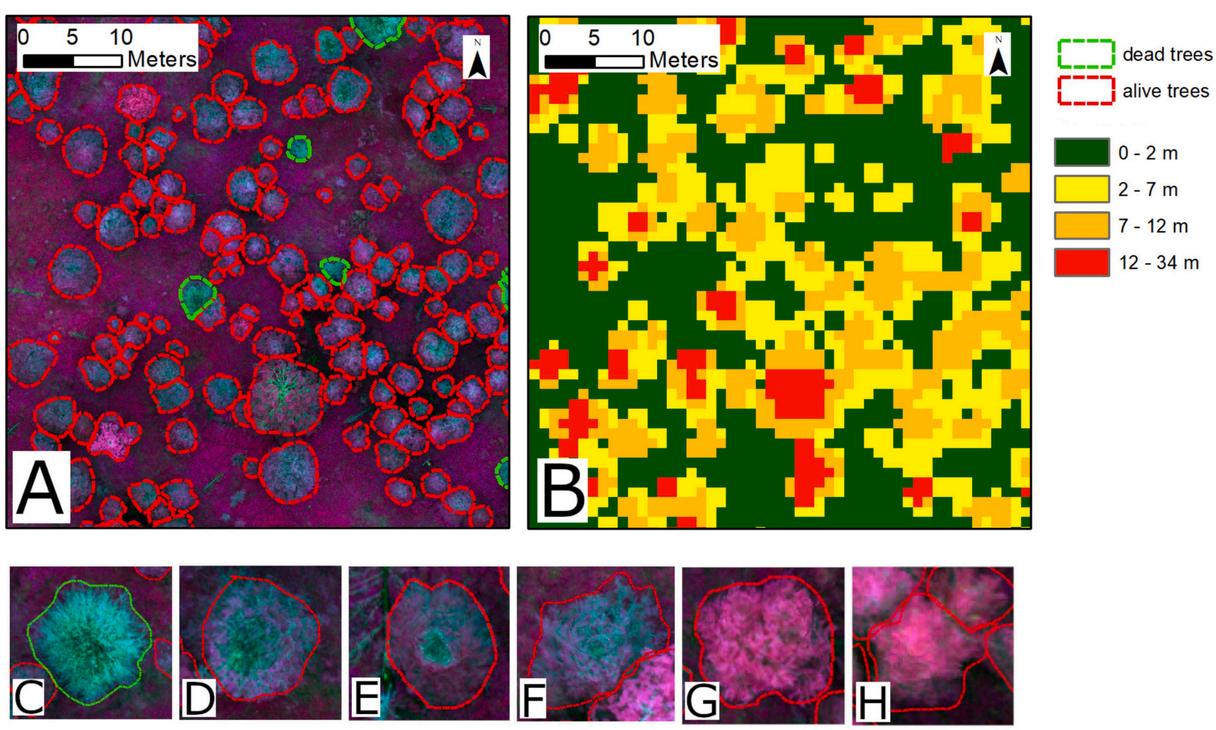

Fig. 4. Two types of input data were used for modelling. Image A shows the polygons of dead and alive tree classes on a false-coloured multispectral image with a 5.2 cm GSD and Image B shows the Canopy Heigh Model with 1 m resolution. The bottom row showcases one dead tree (Image C) and different instances of alive trees classes. Image D and E have dead treetops, while the Image F shows an alive tree with numerous dead branches. Image G and H are examples of alive trees without any major dead parts.

mapping allows explicit spatial monitoring of dead trees as indicators. The U-Net architecture follows a symmetric encoder and decoder structure (Fig. 5). The encoder path consists of five sequential Convolutional Block modules, each followed by a *MaxPool2d* layer to progressively reduce spatial dimensions and capture contextual features. Each Convolutional Blocks include two convolutional layers (with kernel size 3 and padding 1), each followed by batch normalization and *ReLU* activation. Dropout is applied after each activation to mitigate

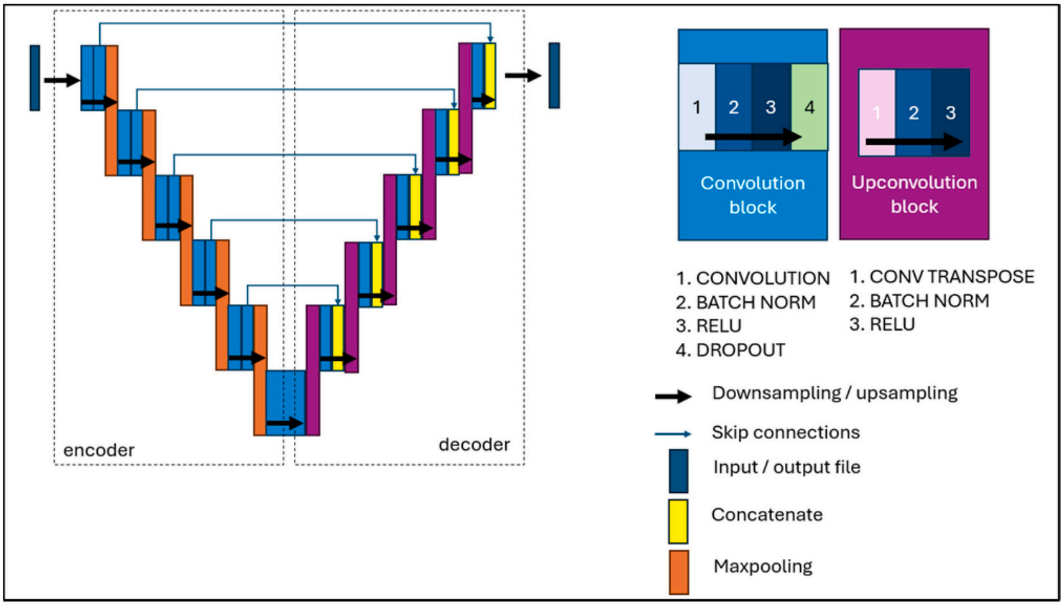

Fig. 5. Schematic overview of the U-Net architecture used in this study.

overfitting, with dropout rates increasing at deeper levels of the encoder. A dropout of 0.0, 0.05, 0.1, 0.15, 0.2, 0.3 were applied for the encoder levels and at the bottleneck. The bottleneck layer further processes the deepest features using a Convolutional Block with the highest number of filters and dropout. The decoder path mirrors the encoder, using *ConvTranspose2d* layers for up-sampling, followed by Convolutional Block modules that refine the concatenated features from the corresponding encoder layers (via skip connections). These skip connections help preserve spatial information lost during down-sampling. The final output is produced by a 1 × 1 convolutional layer that maps the features to the desired number of output classes.

The U-Net model was trained on 256 × 256 pixels input tiles composed of 6-band composites along with reference tree mask files. Training hyperparameters included a learning rate of 0.00001 (higher rates such as 0.001 and 0.0001 were tested but underperformed), 200 epochs (with optimal performance typically between epochs 160–190), and a batch size of 16 (larger sizes like 32 degraded performance). Alternative image sizes (128 and 512) were also tested, but 256 provided the best balance between spatial context and computational efficiency. To address class imbalance (e.g. lot more alive trees and background than dead trees) in the reference masks, we used a *CrossEntropyLoss* function with inverse frequency weighting.

The U-Net model was implemented using Python 3.12, with the core deep learning framework based on PyTorch. Supporting libraries included Rasterio, NumPy, and scikit-learn for evaluation metrics.

2.6. Evaluation of the U-Net model performance

The model output was in the form of logits corresponding to the defined classes. The Model's performance was evaluated using multiple metrics, including F1-score, accuracy, precision, and recall (Eqs. 1–4). The model was trained at the pixel level and evaluated on tree level. Model training was conducted using 10-fold cross-validation, with 90% of the data used for training in each fold and 10% for validation. We considered tree segments classified dead, alive, or background based on the majority of the pixels in each segment.

We decided against on reporting on all classes so as in other multi-class studies (Schwarz et al., 2023), as the overall accuracy metrics would be very high, 0.99, due to large number of background pixels classified correctly. Instead, we report the accuracy of the models on tree segment level, in this case for class 1 (dead tree segments) and class 2 (alive trees segments) and discard the background class. This approach provides a more meaningful assessment of the model's performance to detect tree mortality.

$$F1 = \frac{2 \times Precision \times Recall}{Precision + Recall} \tag{1}$$

$$Accuracy = \frac{TP + TN}{TP + TN + FP + FN} \tag{2}$$

$$Precision = \frac{TP}{TP + FP} \tag{3}$$

$$Recall = \frac{TP}{TP + FN} \tag{4}$$

where TP : *True Positive*, TN : *True Negative*, FP : *False Positive*, FN : *False Negative.*

2.7. Wall-to-wall map and environmental drivers of tree mortality

To create a wall-to-wall tree mortality map for Välisuo area, we created 256 × 256 pixels tiles (matching the training tile size) and applied the trained U-Net model to predict dead and alive tree pixels across the whole landscape. The mortality predictions were aggregated into 16 m × 16 m grid, and we calculated the percentage of dead tree pixels per grid cell as an indicator of mortality. This grid resolution was selected for several reasons. First, it aligns with existing national forest monitoring and risk products in Finland, facilitating comparison and integration with operational datasets. Second, the cell size provides a balance between ecological relevance and statistical stability, smoothing pixel-level noise while retaining spatial sensitivity to mortality hotspots. In addition, the area-based approach was chosen over the crown-area percentage, because tree density varies substantially across the study area. The tiles over the mire areas may only have a few trees, while in forested areas the tiles can have a few dozens of trees. Using an area-based percentage provides a remote-sensing based indicator for identifying mortality hotspots and supports monitoring at the landscape scale.

Afterwards, we analysed potential environmental drivers of mortality by overlaying the mortality map with spatial layers (e.g. soil type, elevation, depth to water or stand composition in Table 1). Areas with

Table 1
Potential environmental drivers of tree mortality and their connection to tree mortality. Climatic variables (temperature, precipitation, snow load) were derived from the Finnish Meteorological Institute open datasets (Finnish Meteorological Institute, 2025). Forest stand attributes, including dominant tree species, age, height, stem density, and development classes, were obtained from forest inventory grid data provided by the Finnish Forest Centre (Suomen Metsäkeskus, 2018). Terrain variables were calculated from airborne lidar data supplied by the National Land Survey of Finland (National Land Survey of Finland, 2020). Soil and hydrological variables were derived from datasets provided by the Natural Resources Institute Finland (Natural Resources Institute Finland, 2016).

List of drivers	Source of data	Relation to tree mortality
Monthly mean temperature (Jan, July 2023)	FMI	Extreme cold and warm periods may increase stress, the trees susceptibility to pests, affect growth and lead to higher mortality.
Yearly mean precipitation (2023)	FMI – calculated from monthly statistics	Droughts or excessive rainfall/snowfall
Mean annual maximum snow loads (kg m-2) on trees are estimated for the period 1981–2010	FMI	Heavy snow loads can break branches or treetops
Depth to water index (DTW) (2023)	LUKE	Shallow DTW can lead to waterlogging, while deep DTW can cause drought
Snow damage risk index (2017)	LUKE	Higher risk means higher risk to mechanical damage
Wind damage risk index (2017)	LUKE	Higher risk means bigger chance of uprooting or stem breakage
TWI (2016)	LUKE	High TWI means more humid soils which may cause root diseases or instability
Dominant tree species (2018–2019)	Metsäkeskus	Different species have different vulnerability and tolerance to pests, diseases, abiotic stress
Mean age/dbh/volume/ height for all species and separately for *Pinus sylvestris*, *Picea abies* and deciduous trees (2018–2019)	Metsäkeskus	Older and bigger trees may be more susceptible to different stress and for natural mortality
Stem count (2018–2019)	Metsäkeskus	High density can increase competition for resources, making trees more vulnerable to stress and mortality
Development classes (2018–2019)	Metsäkeskus	Resilience varies based on stand density, for example, young stands may resist wind better than mature stands
Slope (2018–2019)	Derived from NLS Lidar data	Steep slopes can increase wind exposure and soil erosion, raising mortality risk
Aspect (2018–2019)	Derived from NLS Lidar data	South facing slopes may experience more drought stress. Different exposure to dominant wind direction
Elevation (2018–2019)	Derived from NLS Lidar data	Higher elevation has more exposure, higher wind and snow accumulation
Fertility classes (2018–2019)	Metsäkeskus	Poor soils limit growth and resilience, making trees more prone to stress and mortality
Soil types (2018–2019)	Metsäkeskus	Soils like clay can cause waterlogging, while sandy soils may lead to drought stress, both affecting mortality

the highest mortality were visualised and compared against these drivers to identify patterns that may explain tree health and mortality.

3. Results

3.1. Tree mortality U-Net model performance

The trained U-Net model provided F1-score of 0.57, 0.96 and 0.95 for dead tree, alive tree and combined (dead tree and alive) weighted average respectively (Table 2). Precision and Recall values were higher for alive tree compared to dead tree. Precision value for alive trees was ~1.00, which means trees that were classified as alive trees, were in fact alive trees. In Välisuo area 116 of the dead trees were correctly identified, while only 15 dead trees were missed (classified as background), and 11 dead trees were classified as alive. The accuracy scores for the whole area were 0.92.

Fig. 6 showcases accurate and inaccurate classification examples. Partially dead trees were not in all cases classified correctly as only their dead branches were identified as dead, not the whole trees (first row, third row). A denser forest structure with one fully dead tree in between has been correctly predicted (second row), like other dead trees were mostly correctly found in other areas too (other rows). In row four the model groups a dead tree with the nearby trees' dead branches incorrectly, making the dead tree larger than it is.

The relatively low precision of the dead tree class indicates that many predicted dead trees are false positives, suggesting confusion with structurally similar canopy elements. This pattern is typical in highly imbalanced classification problems, where improving detection of rare classes often increases false positive rates. Visual observations revealed several reoccurring errors. Detection of dead branches on otherwise living trees were sometimes aggregated into false positive on tree segment level, leading to overestimations. In dense stands, overlapping crowns and complex canopy structures further increased confusion between neighboring trees. All these contributed to overestimating mortality. Although a full quantitative decomposition of error sources was not conducted, the reported precision value (0.44) indicates that more than half of predicted dead trees are false positives. This provides a quantitative basis for interpreting the dominant error type, which is consistent with the observed patterns during visual inspection.

3.2. Model performances in three different forest dominated areas

The *Picea abies* dominated areas had the lowest overall accuracy of 0.90 with F1-scores for dead trees and alive trees as 0.56 and 0.95 respectively (Table 3). The *Pinus sylvestris* and deciduous-dominated areas both had 0.97 overall accuracy. The *Pinus sylvestris* dominated areas had an F1-score of 0.59 for dead trees and 0.99 for alive tree, while for the deciduous dominated areas these metrics are 0.71 and 0.98 respectively. It is important to note that the deciduous areas had the least number of trees among the three areas.

The model distinguished between tree classes with a very high performance for alive trees in all areas. However, early listed challenges of dead tree detection, especially in the *Picea abies* dominated areas where

Table 2
Accuracy assessment and metrics on tree level using U-Net model and the multispectral image and canopy height data.

Classes	Precision	Recall	F1-score	Number of samples
Dead Tree Segments	0.44	0.82	0.57	142
Alive Tree Segments	1.00	0.93	0.96	4238
Weighted average (both classes)	0.98	0.92	0.95	4380
Accuracy			0.92	

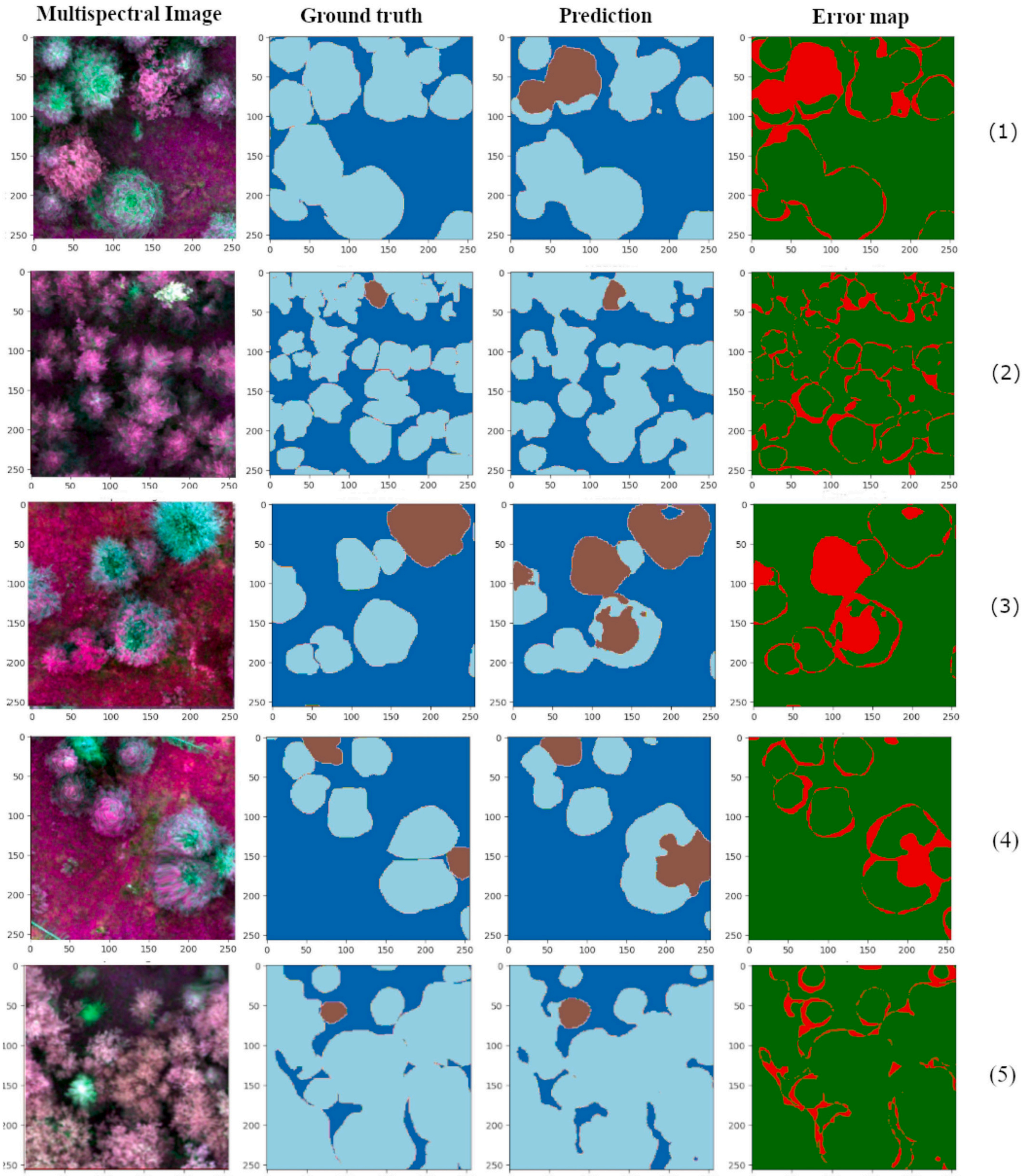

Fig. 6. Examples of correct classification and some common misclassification errors we identified on different forest structures in Välisuo area. (1) shows the misclassification of several partially dead trees; (2) shows a denser forest structure with one fully dead tree (brown) in between alive trees (light blue) over the background (dark blue) that has been correctly predicted; (3) shows a fully dead, correctly classified tree, and other trees were either the treetop or side branches are still alive; however, the model did not assess them as one tree structure in some cases; (4) shows how the model groups a dead tree with the nearby trees' dead branches; (5) shows that the model correctly finds and identifies the dead tree in an area full of deciduous trees. (For interpretation of the references to colour in this figure legend, the reader is referred to the web version of this article.)

Table 3
Comparison of the model's performance on different tree species (*Picea abies*, *Pinus sylvestris*, and deciduous) dominated forest areas. The metrics are counted on tree segment level for both dead and alive trees and their weighted average.

	Picea abies dominated areas			Number of samples	*Pinus sylvestris* dominated areas			Number of samples	Deciduous-dominated areas			Number of trees
	Precision	Recall	F1-score		Precision	Recall	F1-score		Precision	Recall	F1-score	
Dead tree segments	0.42	0.85	0.56	115	0.52	0.68	0.59	19	0.83	0.63	0.71	8
Alive tree segments	1.00	0.90	0.95	2861	1.00	0.97	0.99	1052	0.99	0.98	0.98	325
Weighted average (both classes)	0.97	0.90	0.93	2976	0.99	0.97	0.98	1071	0.99	0.97	0.98	333
Accuracy				0.90				0.97				0.97

there is a clear gap in performance between the two classes. It is worth noting that the *Picea abies* dominated areas had the highest number of dead trees, and the recall was 0.85, the highest recall among the tree areas.

3.3. Wall-to-wall map and potential environmental drivers

The wall-to-wall map shows that the most tree mortality occurred in the southern region of the area (Fig. 7). We acknowledge that the environmental driver analysis is based on classification outputs with moderate reliability for the dead tree class. While aggregation reduces random classification noise, systematic overestimation of mortality (due to false positives) may still bias spatial patterns, which must be considered when interpreting these results. After examining potential environmental drivers (see Table 1) behind mortality (Fig. 8) we found that the area with the highest mortality is where the older and larger *Picea abies* trees (considering both height, basal area, and volume) are located in the southern part of the area in mature, regeneration ready stands. The oldest trees are *Pinus sylvestris* and *Picea abies* in the area, but even though the area dominated by *Pinus sylvestris* has the densest forest structure, the mortality was significantly less in the *Pinus sylvestris* dominated forests grids than in *Picea abies* forests. Based on our visual interpretation of the results, in the *Pinus sylvestris* dominated area, there were no grid cells with over 10% mortality rate, and majority of the grid cells were in the below 5% category, while in the *Picea abies* dominated area there were a large amount of grid cells within the 5–10% mortality rate and eight cells with over 10% mortality rate as well. The snow damage risk map (Fig. 8) also aligns with our findings. Based on visual interpretation of the maps, we found that besides natural mortality, snow damage may be one of the drivers (especially on *Picea abies*) behind the tree mortality in the Välisuo area, particularly affecting *Picea abies* stands which grow on higher elevation, with higher average yearly snow load, consistent with previous studies showing that snow-induced forest damage is common is boreal regions and strongly driven by snow load and stand characteristics (Lehtonen et al., 2014; Suvanto et al., 2021).

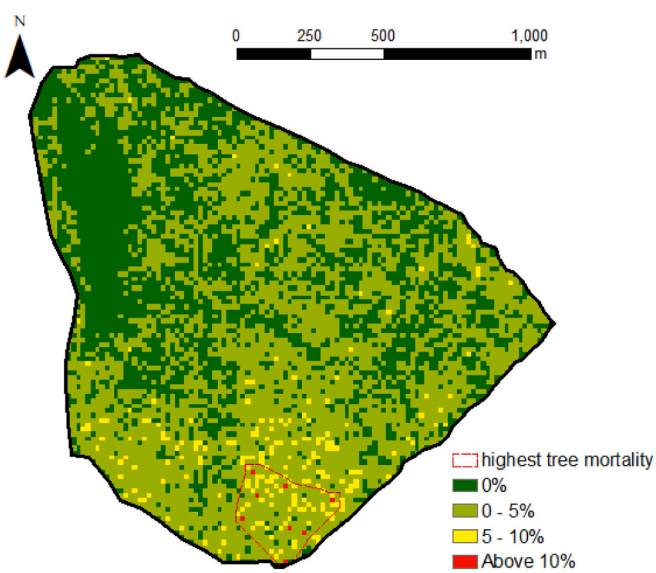

Fig. 7. Dead tree coverage in the Välisuo area (% of the area) displayed on 16 × 16 m grid level. The area with the visually interpreted highest tree mortality marked with the red dotted polygon. (For interpretation of the references to colour in this figure legend, the reader is referred to the web version of this article.)

4. Discussion

4.1. Model performance

The aim of this paper was to evaluate the use of high-resolution UAV images for the detection of tree mortality. This information was then used to assess tree mortality patterns in using a mortality indicator that describes the percentage of dead trees in 16 m × 16 m grid cells in a wall-to-wall fashion in the study area located in Northern Lapland in the Arctic region of Finland. This was achieved by mapping standing dead trees from multispectral UAV imagery combined with lidar derived canopy height data using a U-Net based deep learning approach. Classical methods typically depend on explicitly defined features and pre-segmented objects, which are sensitive to illumination, acquisition settings, and forest structure. The use of U-Net therefore provides a more transferable framework for large-area, multi-class mortality mapping.

Our model achieved 0.92 overall accuracy, with high performance for alive tree segments (F1 = 0.96) and moderate performance for dead tree segments (F1 = 0.57). Under strong class imbalance, overall accuracy can be misleading; for example, a classifier assigning all trees as alive would achieve high accuracy but fail to detect mortality. Therefore, the higher recall obtained in this study represents a meaningful improvement despite lower precision. The moderate F1-scores for dead trees primarily reflect an imbalance between high recall (0.63–0.85) and low 0.42–0.83 precision, indicating that most dead trees were successfully detected, but the model resulted in many false positives. These false positives were mainly associated with partially dead tree crowns, the presence of dead branches within the otherwise living trees, and overlapping canopies in denser *Picea abies* dominated stands, where individual crown boundaries are sometimes difficult to delineate consistently. Shadows further increased the spectral ambiguity. Such errors are typical in high-resolution optical mortality mapping and are trade-offs between sensitivity and precision in multi-class segmentation. Accuracy varied across forest types, with the *Picea abies* dominated area showing the lowest performance (0.90), which is consistent with its higher mortality rate and more complex canopy structure, which is characterized by dense crown overlap, multi-layered canopies, and irregular crown shapes.

Compared with recent UAV and aerial imagery based deep learning studies, our results fall in the similar accuracy range. Binary classification, e.g. healthy vs. dead or damaged classification often achieves F1

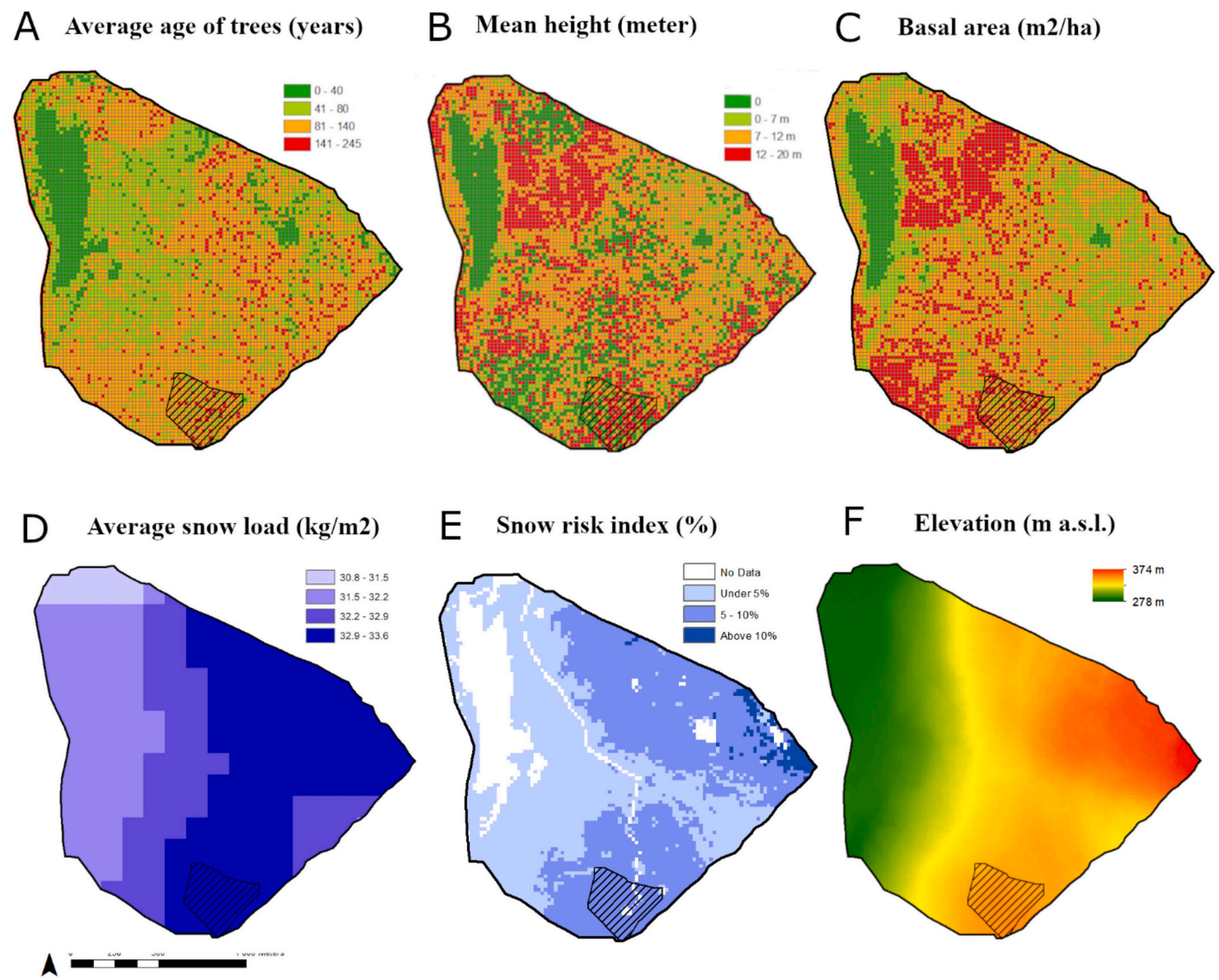

Fig. 8. Tree mortality and potential environmental and geographical drivers. The area marked by strips is the area with the highest mortality.

scores over 0.85 (Anwander et al., 2024; Schiefer et al., 2023; Zhou et al., 2024), while multi-class classification and landscape-wide segmentation tasks typically report lower accuracy. Schiefer et al. (2023) used comparative resolution to our study, 4 cm, and achieved an F1 score of 0.85 for a simpler binary classification of dead trees over background with an overall precision of 0.90 and recall of 0.85, which are slightly higher than our multi-class results. Junttila et al. (2024) achieved an F1 score of 0.86–0.93, however their assessment of results differs from ours. We chose a more moderate approach to assess our results, and we considered dead or alive tree correctly classified if the majority of pixels within belonged to the correct class, however, in Junttila's work even one dead tree pixel within the dead tree polygon meant that the results are correct. Important to note also that the resolution was lower, 0.5 m.

The relatively low precision of the dead tree class indicates that many predicted mortality signals correspond to structurally complex but living canopy elements. Compared to previous studies, the model achieves comparable recall but lower precision, highlighting an inherent trade-off in detecting rare classes such as dead trees. This trade-off reflects the difficulty of distinguishing fully dead trees from partially defoliated or shaded crowns using remote sensing data (Rahman et al., 2025). As such, the model is not suitable for operational decision-making at the individual tree or stand level without validation. High false positive rates may lead to inefficient field verification and limit user trust, which constrains practical operational deployment. Instead, its main utility lies in identifying areas with elevated likelihood of mortality, which can support targeted field surveys.

Our three-class model's performance is comparable to other multi-class approaches (Gonzalez and Wallner, 2025; Schwarz et al., 2023), even though out study doesn't omit ambiguous crowns or undetected objects prior to classification which are common in instance-based (e.g. YOLO) methods. Schwarz et al. (2023) used 20 cm GSD tiles with an F1 score of 0.66–0.71 excluding the background, and F1 score of 0.99 including it. Our Model has comparable results, in some areas performing slightly better, and in other areas slightly worse. Gonzalez and Wallner (2025) also used 20 cm pixel size on their training data, and the results varied a lot from poorly performing models to the best performing Attention U-Net which had an F1-score of 0.68 for multi-class classification and 0.72 for binary. Studies in more southern areas of Finland (Mäyrä et al., 2021, 2025) showed mean average precision at IoU at 50% (mAP50) showed 0.65–0.68 while in tree species recognition an F1 scores over 0.80. Intersection over Union (IoU) measures the spatial overlap between predicted and reference tree segments, while mean Average Precision at an IoU threshold of 50% (mAP50) summarizes detection performance by considering predictions with at least 50% overlap as correct.

Our approach of classifying each pixel then assessing segments creates object level information with a scalable approach for mortality mapping, even though single-tree models may achieve higher precision under simplified class definitions or validation methods.

4.2. Environmental drivers for tree mortality

The mortality hotspots were concentrated in the southern, higher elevation parts of the study area, dominated by of older and larger *Picea abies* tree stands. These stands consist of mature; regeneration tree stands. After examining the potential drivers,

After examining the potential drivers, we observed that *Pinus sylvestris* dominated stands exhibited lower mortality levels than *Picea abies* dominated stands, despite having high stand density and comparable or greater mean tree height and basal area (Table 3; Figs. 7–8). Mortality hotspots were primarily concentrated in mature *Picea abies* stands located at higher elevations, where snow-damage risk was also elevated. These patterns are consistent with established ecological understanding that shallow-rooted *Picea abies* is particularly vulnerable to mechanical damage under heavy snow loads in boreal conditions (Nykänen et al., 1997; Lehtonen et al., 2014), and that older stands are generally more susceptible to abiotic stress and secondary disturbances such as pest outbreaks (Netherer et al., 2024).

Other environmental drivers are the precipitation e.g. snowfall and snow load. The 2017–2018 winter season in Finland had an exceptionally high snowfall and cumulative snow-load. The national 16 m grid level snow-damage risk map (Suvanto et al., 2021) aligns with our findings that snow load, elevation and exposure are the key environmental drivers (Suvanto et al., 2021; Tomppo et al., 2019). On broader scale, canopy mortality increased consistently since the mid-1980s (Senf et al., 2018, 2021), reflecting intensification of the climate related disturbances while reshaping forest demography toward younger age classes, and impacting biodiversity and carbon storage. These trends had an amplified effects in the Arctic (Rantanen et al., 2022), urging for a scalable mortality indicator in boreal and Arctic regions.

4.3. Implication for tree mortality detection method development

We used a three-class division (alive, dead, and background) to balance ecological relevance with operational feasibility. More detailed health classes such as partially dead or disease-infected are ecologically meaningful but difficult to validate consistently at landscape scale without repeated field inventories. Recent study shows that often expanding the number of classes lowers the performance significantly compared to binary classification and demands intensive field work (Anwander et al., 2024). Our approach prioritises scalability, field verifiability, and future integration with landscape-level monitoring.

The method still has several uncertainties and limitations. Partial mortality, e.g. dead tops or branches, and under-canopy mortality can cause misclassification and under detection in optical nadir imagery (Junttila et al., 2024; Schiefer et al., 2023). To reduce misclassification, in our training data we considered only 3 classes, merging all partially dead tree with the alive ones. However, not mapping partial mortality as a separate category has its own limitation for the proposed approach. In forests affected by climate-driven stress, such intermediate states are common; however, the present workflow is intentionally designed to detect only fully dead standing trees. This choice aligns with biodiversity monitoring objectives, where standing deadwood is the primary indicator of interest, and supports scalability and clear interpretation of the results. Seasonal factors, such as leaf-on and leaf-off data and snow cover influence spectral separability among different classes. We also acknowledge that detecting only fully dead trees limits the method's ability to function as an early warning system. Partial crown mortality represents an earlier stage of decline; however, it is also more difficult to detect reliably using remote sensing data. Future work should explicitly target gradient-based mortality detection to better capture early-stage decline.

Manual crown delineation is another source of uncertainty, especially in dense forest stand where crown boundaries overlap. Post-processing, e.g. watershed or attention modules, may reduce these artifacts but not eliminate them (Zhou et al., 2024). The sample size, especially for dead tree crowns, was relatively small in our study for a deep learning method. This can bias the model toward the majority class, the alive trees, while the recall of dead trees remains lower, as observed particularly in *Pinus sylvestris* and deciduous dominated areas. More robust and diverse training data are needed to ensure the model handles dead trees reliably, as their appearance varies widely with species, crown structure, and decay stage. Without capturing this variability, the model may not generalize well to other sites, disturbance types, or mortality conditions. Beyond monitoring dead trees, the mortality indicator which expresses the percentage of dead trees in a 16 m × 16 m area, also supports biodiversity assessments. Deadwood is a widely recognised biodiversity indicator and strongly associated with species richness among decomposing fungi, beetles and cavity nesting birds (Humphrey et al., 2005; Lassauce et al., 2011). In Finland, many red-listed species are associated with deadwood, notably in *Picea abies* and European Aspen (*Populus tremula* L.) habitats (Rana et al., 2024; Tikkanen et al., 2006). By mapping mortality hotspots and quantifying mortality intensity, our indicator provides a spatial tool to support deadwood retention strategies, prioritize mixed and climate smart forestry.

The transferability of the model depends on the availability and acquisition of high-resolution imagery and low-pulse-density lidar data. A key strength of the workflow is the integration of national airborne lidar-derived CHMs, which provide consistent structural information across large areas in Finland. However, such nationally harmonized lidar products are not universally available, limiting direct transferability to regions lacking comparable reference data. Consequently, the current approach is most readily applicable in countries with systematic national lidar coverage, such as Finland and Sweden. In addition, model performance may be influenced by variations in acquisition conditions, including seasonal illumination, snow cover, and UAV flight parameters (e.g., altitude, sensor configuration, and viewing geometry). These factors can affect both spectral response and crown delineation, particularly in boreal environments with strong seasonal variation. Although the use of height-based information contributes to robustness, adapting the model to new regions or acquisition settings would likely require region-specific retraining or normalization strategies.

Disturbances occurring after shortly data acquisition may cause inconsistencies when trees have fallen or regenerated between datasets. However, with suitable imagery and training data the method can help fill spatial and temporal gaps in traditional monitoring systems, particularly after bark beetle outbreaks, drought-related mortality, or extreme snow damage (Senf et al., 2021) Moreover, multi-temporal assessments can aid and create more robust predictions and offer a near real-time support for forest managers post-disturbances.

Overall, the presented approach demonstrates the potential of deep learning for large-area mortality mapping but remains limited by classification uncertainty, particularly for the dead tree class. Our wall-to-wall mapping can be used as preliminary planning tool, rather than a fully operational monitoring system at its current state, to helps identifying stress hotspots and aligns with European and international monitoring need (European Commission, 2021; Forest Europe, 2020; United Nations, 2023). The results should therefore be interpreted as exploratory indicators of spatial mortality patterns rather than precise maps of individual dead trees. Future work should focus on improving class separability, incorporating temporal information, and explicitly addressing partial mortality to enhance both precision and operational relevance.

5. Conclusion

Our study demonstrates that U-Net-based segmentation combined with high resolution aerial imagery and lidar-derived canopy height models data can provide a scalable and spatially quantifiable indicator for tree mortality. In the Arctic region, forest health and tree mortality are typically assessed using field plot data with limited spatial coverage, despite the rapid environmental changes driven by climate change. Our results show that the proposed approach can reliably identify alive trees and detect dead trees with high recall but substantial uncertainty due to false positives. The indicator was not solely aimed only at precise tree-level mortality accounting, but also for spatially explicit identification of mortality patterns and hotspots. By detecting dead tree hotspots and linking them to key environmental drivers such as elevation, snow load, and forest stand structure, the indicator can support preliminary assessment of mortality patterns, but does not yet provide a reliable early-warning capability, It can complement forest inventories in future, strengthening its value for biodiversity assessments and climate-resilient forest management. Future research should focus on extending this approach to Sentinel-2 satellite-based observations to enable large scale and continuous monitoring of tree mortality with a 5-day revisit time. Integrating UAV based high resolution products with Sentinel-2 10–20 m resolution data-based time series could support model transferability and temporal monitoring of mortality dynamics.

CRediT authorship contribution statement

Katalin Waga: Writing – review & editing, Writing – original draft, Visualization, Validation, Methodology, Formal analysis, Conceptualization. **Jaan Rönkkö:** Writing – review & editing, Methodology. **Mikko Kukkonen:** Writing – review & editing, Methodology. **Anton Kuzmin:** Writing – review & editing, Methodology, Data curation. **Timo Kumpula:** Writing – review & editing, Funding acquisition. **Parvez Rana:** Writing – review & editing, Supervision, Methodology, Funding acquisition, Conceptualization.

Declaration of competing interest

The authors declare that they have no known competing financial interests or personal relationships that could have appeared to influence the work reported in this paper.

Acknowledgements

This work was funded by European Regional Development Fund (ERDF) Interreg Aurora programme (RESONATE project, grant number: 20366456), and Research Council of Finland (grant number 347862).

Appendix A. Appendix

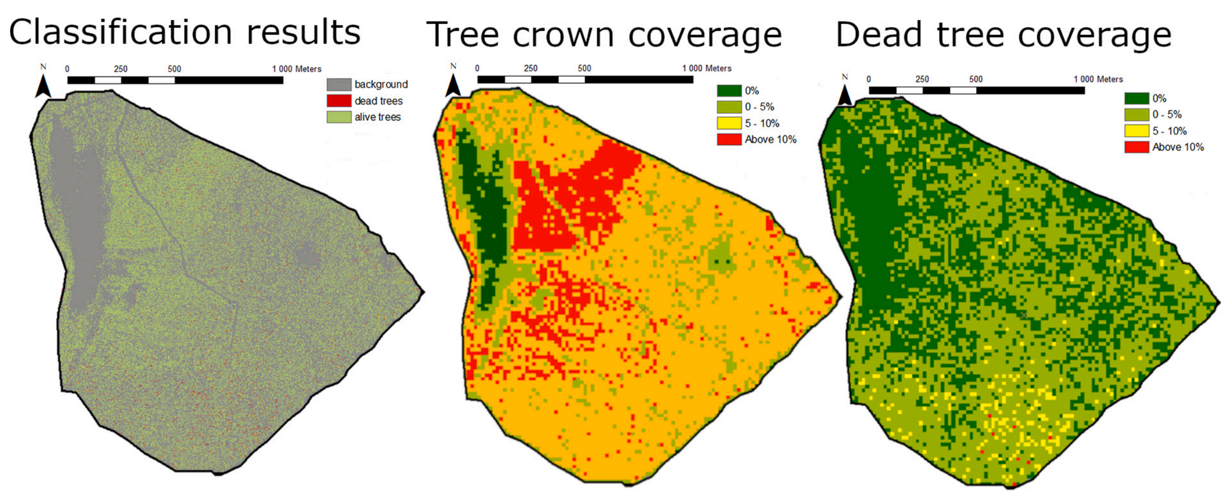

Fig. 9. Pixel-level classification (left), tree crown coverage (middle) and dead tree coverage - tree mortality predictions (right) on wall-to-wall maps of Välisuo area. The 3-class pixel level classification shows how each pixel is assigned one of the tree classes: dead tree, alive tree, or background (not a tree). The other two maps show percentages of the total area covered by any trees (middle) and by dead trees (right) are shown in 16 m × 16 m squares.

Data availability

The training data and methods may be available upon request.

References

Anwander, J., Brandmeier, M., Paczkowski, S., Neubert, T., Paczkowska, M., 2024. Evaluating different deep learning approaches for tree health classification using high-resolution multispectral UAV data in the Black Forest, Harz region, and Göttinger Forest. Remote Sens. 16 (3). https://doi.org/10.3390/rs16030561.

Bergmüller, K.O., Vanderwel, M.C., 2022. Predicting tree mortality using spectral indices derived from multispectral UAV imagery. Remote Sens. 14 (9). https://doi.org/10.3390/rs14092195.

Biedermann, P.H.W., Müller, J., Grégoire, J.-C., Gruppe, A., Hagge, J., Hammerbacher, A., Hofstetter, R.W., Kandasamy, D., Kolarik, M., Kostovcik, M., Krokene, P., Sallé, A., Six, D.L., Turrini, T., Vanderpool, D., Wingfield, M.J., Bässler, C., 2019. Bark beetle population dynamics in the Anthropocene: challenges and solutions. Trends Ecol. Evol. 34 (10), 914–924. https://doi.org/10.1016/j.tree.2019.06.002.

Cajander, A.K., 1926. The theory of forest types. Acta For. Fenn. 29 (3). https://doi.org/10.14214/aff.7193.

Chapin, F.S., McGuire, A.D., Ruess, R.W., Hollingsworth, T.N., Mack, M.C., Johnstone, J. F., Kasischke, E.S., Euskirchen, E.S., Jones, J.B., Jorgenson, M.T., Kielland, K., Kofinas, G.P., Turetsky, M.R., Yarie, J., Lloyd, A.H., Taylor, D.L., 2010. Resilience of Alaska's boreal forest to climatic changeThis article is one of a selection of papers from the dynamics of change in Alaska's boreal forests: resilience and vulnerability in response to climate warming. Can. J. For. Res. 40 (7), 1360–1370. https://doi.org/10.1139/x10-074.

Christiani, P., Isoaho, A., Elo, M., Päkkilä, L., Marttila, H., Aalto, J., Hjort, J., Tolvanen, A., Rana, P., Räsänen, A., 2025. Negative effects of climate warming on red-listed boreal peatland plant species can be mitigated through restoration. Biol. Conserv. 306, 111126. https://doi.org/10.1016/j.biocon.2025.111126.

European Commission, 2021. New EU Forest strategy for 2030. https://commission.europa.eu/document/cf3294e1-8358-4c93-8de4-3e1503b95201_en.

European commission, 2024. Nature Restoration Regulation- EU Biodiversity Strategy. https://environment.ec.europa.eu/topics/nature-and-biodiversity/nature-restoration-regulation_en.

Finnish Meteorological Institute, 2025. FMI Open Data [Dataset]. https://en.ilmatieteenlaitos.fi/open-data.

Ford, K.R., Breckheimer, I.K., Franklin, J.F., Freund, J.A., Kroiss, S.J., Larson, A.J., Theobald, E.J., HilleRisLambers, J., 2017. Competition alters tree growth responses to climate at individual and stand scales. Can. J. For. Res. 47 (1), 53–62. https://doi.org/10.1139/cjfr-2016-0188.

Forest Europe, former M. C. on the P. of F. in E, 2020. State of Europe's Forests 2020. Ministerial Conference on the Protection of Forests in Europe - FOREST EUROPE. https://foresteurope.org/wp-content/uploads/2016/08/SoEF_2020.pdf.

Francis, E.J., Jung, C.G., Hicke, J.A., Hurteau, M.D., 2025. Modeling the probability of bark beetle-caused tree mortality as a function of watershed-scale host species presence and basal area. For. Ecol. Manage. 580, 122549. https://doi.org/10.1016/j.foreco.2025.122549.

Gonzalez, J.F., Wallner, A., 2025. Robust U-net segmentation of tree crown damages in Bavaria, Germany. Eng. Proc. 94 (1). https://doi.org/10.3390/engproc2025094012.

Han, Z., Hu, W., Peng, S., Lin, H., Zhang, J., Zhou, J., Wang, P., Dian, Y., 2022. Detection of standing dead trees after pine wilt disease outbreak with airborne remote sensing imagery by multi-scale spatial attention deep learning and gaussian kernel approach. Remote Sens. 14 (13). https://doi.org/10.3390/rs14133075.

Hart, S.J., Veblen, T.T., 2015. Detection of spruce beetle-induced tree mortality using high- and medium-resolution remotely sensed imagery. Remote Sens. Environ. 168, 134–145. https://doi.org/10.1016/j.rse.2015.06.015.

Humphrey, J.W., Ylisirniö, A.-L., Lemperiere, G., Dodelin, B., Alexander, K., Butler, J.E., 2005. Deadwood as an indicator of biodiversity in European forests: From theory to operational guidance, 51, pp. 193–206.

Junttila, S., Blomqvist, M., Laukkanen, V., Heinaro, E., Polvivaara, A., O'Sullivan, H., Yrttimaa, T., Vastaranta, M., Peltola, H., 2024. Significant increase in forest canopy mortality in boreal forests in Southeast Finland. For. Ecol. Manage. 565, 122020. https://doi.org/10.1016/j.foreco.2024.122020.

Kanerva, H., Honkavaara, E., Näsi, R., Hakala, T., Junttila, S., Karila, K., Koivumäki, N., Alves Oliveira, R., Pelto-Arvo, M., Pölönen, I., Tuviala, J., Östersund, M., Lyytikäinen-Saarenmaa, P., 2022. Estimating tree health decline caused by *Ips typographus* L. from UAS RGB images using a deep one-stage object detection neural network. Remote Sens. *14* (24). https://doi.org/10.3390/rs14246257.

Keränen, K., Isoaho, A., Räsänen, A., Hjort, J., Kumpula, T., Korpelainen, P., Rana, P., 2024. Multi-resolution remote sensing for flark area detection in boreal aapa mires. Int. J. Remote Sens. 45 (13), 4324–4343. https://doi.org/10.1080/01431161.2024.2359732.

Kharuk, V.I., Petrov, I.A., Krivobokov, L.V., Golyukov, A.S., Dvinskaya, M.L., Im, S.T., Shushpanov, A.S., Smith, K.T., 2022. Larch response to warming in northern Siberia. Reg. Environ. Chang. 23 (1), 17. https://doi.org/10.1007/s10113-022-02016-9.

Khosravipour, A., Skidmore, A., Isenburg, M., Hussin, Y., 2014. Generating pit-free canopy height models from airborne lidar. Photogramm. Eng. Remote Sens. 80, 863–872. https://doi.org/10.14358/PERS.80.9.863.

Kosolapova, A., Altshuler, I., 2024. Effects of reduced snowpack due to climate warming on abiotic and biotic soil properties in alpine and boreal forest systems. PLOS Climate 3 (5), e0000417. https://doi.org/10.1371/journal.pclm.0000417.

Kretschmann, D., 2010. Mechanical properties of wood. In: Wood Handbook: Wood as an Engineering Material*:* Chapter 5. https://research.fs.usda.gov/treesearch/37427.

Kuzmin, A., Korhonen, L., Tanhuanpää, T., Kukkonen, M., Maltamo, M., Kumpula, T., 2026. Classification of tree species and standing dead trees in boreal forests using UAV-based RGB, multispectral, and LiDAR point clouds. Remote Sensing of Ecology and (Conservation). ISSN 2056-3485 (electronic), 1–16. https://doi.org/10.1002/rse2.70070.

Lassauce, A., Paillet, Y., Jactel, H., Bouget, C., 2011. Deadwood as a surrogate for forest biodiversity: Meta-analysis of correlations between deadwood volume and species richness of saproxylic organisms. Ecol. Indic. 11 (5), 1027–1039. https://doi.org/10.1016/j.ecolind.2011.02.004.

Lehtonen, I., Hoppula, P., Pirinen, P., Gregow, H., 2014. Modelling crown snow loads in Finland: a comparison of two methods. Silva Fenn. 48 (3). https://doi.org/10.14214/sf.1120.

Liu, M., Trugman, A., Penuelas, J., Anderegg, W., 2024. Climate-driven disturbances amplify forest drought sensitivity. Nat. Clim. Chang. 14. https://doi.org/10.1038/s41558-024-02022-1.

Martinez del Castillo, E., Torbenson, M., Reinig, F., Tejedor, E., de Luis, M., Esper, J., 2024. Contrasting future growth of Norway spruce and Scots pine forests under warming climate. Glob. Chang. Biol. 30, e17580. https://doi.org/10.1111/gcb.17580.

Martz, F., Vuosku, J., Ovaskainen, A., Stark, S., Rautio, P., 2016. The snow must go on: ground ice encasement, snow compaction and absence of snow differently cause soil hypoxia, CO2 accumulation and tree seedling damage in boreal Forest. PloS One 11 (6), e0156620. https://doi.org/10.1371/journal.pone.0156620.

Mäyrä, J., Keski-Saari, S., Kivinen, S., Tanhuanpää, T., Hurskainen, P., Kullberg, P., Poikolainen, L., Viinikka, A., Tuominen, S., Kumpula, T., Vihervaara, P., 2021. Tree species classification from airborne hyperspectral and LiDAR data using 3D convolutional neural networks. Remote Sens. Environ. 256, 112322. https://doi.org/10.1016/j.rse.2021.112322.

Mäyrä, J., Tanhuanpää, T., Kuzmin, A., Heinaro, E., Kumpula, T., Vihervaara, P., 2025. Using UAV images and deep learning to enhance the mapping of deadwood in boreal forests. Remote Sens. Environ. 329, 114906. https://doi.org/10.1016/j.rse.2025.114906.

McIlroy, S., Shinneman, D., 2020. Post-fire aspen (*Populus tremuloides*) regeneration varies in response to winter precipitation across a regional climate gradient. Forest Ecol. Manage. 455. https://doi.org/10.1016/j.foreco.2019.117681. USGS Publications Warehouse.

Mudryk, L.R., Elias Chereque, A., Derksen, C., Luojus, K., Decharme, B., 2024. NOAA arctic report card 2024: terrestrial snow cover. In: NOAA Technical Report OAR ARC. https://doi.org/10.25923/4bb3-3f87, 24–04 (Arctic Report Card). (noaa: 66841).

National Land Survey of Finland, 2020. Laser Scanning Data 0.5 p [Dataset]. https://www.maanmittauslaitos.fi/en/maps-and-spatial-data/datasets-and-interfaces/product-descriptions/laser-scanning-data-05-p.

Natural Resources Institute Finland, 2016. Soil Database [Dataset]. https://paituli.csc.fi/download.html.

Netherer, S., Lehmanski, L., Bachlehner, A., Rosner, S., Savi, T., Schmidt, A., Huang, J., Paiva, M.R., Mateus, E., Hartmann, H., Gershenzon, J., 2024. Drought increases Norway spruce susceptibility to the Eurasian spruce bark beetle and its associated fungi. New Phytol. 242 (3), 1000–1017. https://doi.org/10.1111/nph.19635.

Nykänen, M.-L., Peltola, H., Quine, C.P., Kellomäki, S., Broadgate, M., 1997. Factors affecting snow damage of trees with particular reference to European conditions. Silva Fenn. 31 (2). https://doi.org/10.14214/sf.a8519.

Pakalne, M., 2025. Life PeatCarbon project: the role of peatlands for climate change mitigation. Open access government 430–431. October.

Parajuli, R., Markwith, S., 2023. Quantity is foremost but quality matters: a global meta-analysis of correlations of dead wood volume and biodiversity in forest ecosystems. Biol. Conserv. 283, 110100. https://doi.org/10.1016/j.biocon.2023.110100.

Patacca, M., Lindner, M., Lucas-Borja, M.E., Cordonnier, T., Fidej, G., Gardiner, B., Hauf, Y., Jasinevičius, G., Labonne, S., Linkevičius, E., Mahnken, M., Milanovic, S., Nabuurs, G.-J., Nagel, T.A., Nikinmaa, L., Panyatov, M., Bercak, R., Seidl, R., Ostrogović Sever, M.Z., Schelhaas, M.-J., 2023. Significant increase in natural disturbance impacts on European forests since 1950. Glob. Chang. Biol. 29 (5), 1359–1376. https://doi.org/10.1111/gcb.16531.

Prieur, J.-F., St-Onge, B., Fournier, R.A., Woods, M.E., Rana, P., Kneeshaw, D., 2022. A comparison of three airborne laser scanner types for species identification of individual trees. Sensors 22 (1). https://doi.org/10.3390/s22010035.

Puliti, S., Lines, E.R., Müllerová, J., Frey, J., Schindler, Z., Straker, A., Allen, M.J., Winiwarter, L., Rehush, N., Hristova, H., Murray, B., Calders, K., Coops, N., Höfle, B., Irwin, L., Junttila, S., Krůček, M., Krok, G., Král, K., Astrup, R., 2025. Benchmarking tree species classification from proximally sensed laser scanning data: introducing the FOR-species20K dataset. Methods Ecol. Evol. 16 (4), 801–818. https://doi.org/10.1111/2041-210X.14503.

Rahman, A.U., Heinaro, E., Ahishali, M., Junttila, S., 2025. Dual-task learning for dead tree detection and segmentation with hybrid self-attention U-Nets in aerial imagery. Int. J. Appl. Earth Obs. Geoinf. 144, 104851. https://doi.org/10.1016/j.jag.2025.104851.

Rana, P., Tolvanen, A., 2021. Transferability of 34 red-listed peatland plant species models across boreal vegetation zone. Ecol. Indic. 129, 107950. https://doi.org/10.1016/j.ecolind.2021.107950.

Rana, P., St-Onge, B., Prieur, J.-F., Cristina Budei, B., Tolvanen, A., Tokola, T., 2022. Effect of feature standardization on reducing the requirements of field samples for individual tree species classification using ALS data. ISPRS J. Photogramm. Remote Sens. 184, 189–202. https://doi.org/10.1016/j.isprsjprs.2022.01.003.

Rana, P., Christiani, P., Ahtikoski, A., Haikarainen, S., Stenberg, L., Juutinen, A., Tolvanen, A., 2024. Cost-efficient management of peatland to enhance biodiversity in Finland. Sci. Rep. 14 (1), 2489. https://doi.org/10.1038/s41598-024-52964-x.

Rantanen, M., Karpechko, A.Yu., Lipponen, A., Nordling, K., Hyvärinen, O., Ruosteenoja, K., Vihma, T., Laaksonen, A., 2022. The Arctic has warmed nearly four times faster than the globe since 1979. Commun. Earth Environ. 3 (1), 168. https://doi.org/10.1038/s43247-022-00498-3.

Redmon, J., Divvala, S., Girshick, R., Farhadi, A., 2016. You only look once: unified, real-time object detection, p. 788. https://doi.org/10.1109/CVPR.2016.91.

Robbins, Z.J., Xu, C., Aukema, B.H., Buotte, P.C., Chitra-Tarak, R., Fettig, C.J., Goulden, M.L., Goodsman, D.W., Hall, A.D., Koven, C.D., Kueppers, L.M., Madakumbura, G.D., Mortenson, L.A., Powell, J.A., Scheller, R.M., 2021. Warming increased bark beetle-induced tree mortality by 30% during an extreme drought in California. Glob. Chang. Biol. 28 (2), 509–523. https://doi.org/10.1111/gcb.15927.

Ronneberger, O., Fischer, P., Brox, T., 2015. U-net: Convolutional networks for biomedical image segmentation. In: Navab, N., Hornegger, J., Wells, W.M., Frangi, A.F. (Eds.), Medical Image Computing and Computer-Assisted Intervention – MICCAI 2015. Springer International Publishing, pp. 234–241.

Schiefer, F., Schmidtlein, S., Frick, A., Frey, J., Klinke, R., Zielewska-Büttner, K., Junttila, S., Uhl, A., Kattenborn, T., 2023. UAV-based reference data for the prediction of fractional cover of standing deadwood from sentinel time series. ISPRS Open Journal of Photogrammetry and Remote Sensing 8, 100034. https://doi.org/10.1016/j.ophoto.2023.100034.

Schwarz, S., Werner, C., Fassnacht, F.E., Ruehr, N.K., 2023. Forest canopy mortality during the 2018-2020 summer drought years in Central Europe: the application of a deep learning approach on aerial images across Luxembourg. Forestry: An International Journal of Forest Research 97 (3), 376–387. https://doi.org/10.1093/forestry/cpad049.

Senf, C., Pflugmacher, D., Zhiqiang, Y., Sebald, J., Knorn, J., Neumann, M., Hostert, P., Seidl, R., 2018. Canopy mortality has doubled in Europe's temperate forests over the last three decades. Nat. Commun. 9. https://doi.org/10.1038/s41467-018-07539-6.

Senf, C., Sebald, J., Seidl, R., 2021. Increasing canopy mortality affects the future demographic structure of Europe's forests. One Earth 4 (5), 749–755. https://doi.org/10.1016/j.oneear.2021.04.008.

Singh, V.V., Naseer, A., Mogilicherla, K., Trubin, A., Zabihi, K., Roy, A., Jakuš, R., Erbilgin, N., 2024. Understanding bark beetle outbreaks: exploring the impact of changing temperature regimes, droughts, forest structure, and prospects for future

forest pest management. Rev. Environ. Sci. Biotechnol. 23 (2), 257–290. https://doi.org/10.1007/s11157-024-09692-5.
Slepetiene, A., Belova, O., Fastovetska, K., Dinca, L., Murariu, G., 2025. Managing boreal birch forests for climate change mitigation. Land 14 (9), 1909. https://doi.org/10.3390/land14091909.
Sun, Z., Wang, X., Wang, Z., Yang, L., Xie, Y., Huang, Y., 2021. UAVs as remote sensing platforms in plant ecology: review of applications and challenges. J. Plant Ecol. 14 (6), 1003–1023. https://doi.org/10.1093/jpe/rtab089.
Suomen Metsäkeskus, 2018. *SMK Open Data (grid data)* [Dataset]. https://avoin.metsakeskus.fi.
Suvanto, S., Lehtonen, A., Nevalainen, S., Lehtonen, I., Viiri, H., Strandström, M., Peltoniemi, M., 2021. Mapping the probability of forest snow disturbances in Finland. PloS One 16 (7), 1–20. https://doi.org/10.1371/journal.pone.0254876.
Sylvain, J.-D., Drolet, G., Brown, N., 2019. Mapping dead forest cover using a deep convolutional neural network and digital aerial photography. ISPRS Journal of Photogrammetry and Remote Sensing 156, 14–26. https://doi.org/10.1016/j.isprsjprs.2019.07.010.
Tikkanen, O.-P., Martikainen, P., Hyvärinen, E., Junninen, K., Kouki, J., 2006. Red-listed boreal forest species of Finland: associations with forest structure, tree species, and decaying wood. Ann. Zool. Fenn. 43, 373–383.
Tomppo, E., Antropov, O., Praks, J., 2019. Boreal forest snow damage mapping using multi-temporal Sentinel-1 data. Remote Sens. 11 (4). https://doi.org/10.3390/rs11040384.
U.S. Forest Service, 2024. In: U.S. Department of Agriculture, Forest Service (Ed.), Armillaria Root Disease in Conifers of Western North America.
United Nations, 1992. Convention on Biological Diversity. https://www.cbd.int/doc/handbook/cbd-hb-01-en.pdf.
United Nations, 2023. Boreal Forests and Climate Change from Impacts to Adaptation—Policy Brief. UN Economic Commission for Europe. https://unece.org/sites/default/files/2023-03/Boreal%20forests%20policy%20brief_%20ENG_final0.pdf.
Way, D.A., Oren, R., 2010. Differential responses to changes in growth temperature between trees from different functional groups and biomes: a review and synthesis of data. Tree Physiol. 30 (6), 669–688. https://doi.org/10.1093/treephys/tpq015.
Xu, S., Huang, W., Wang, D., Zhang, B., Sun, H., Yan, J., Ding, J., Wang, J., Yang, Q., Huang, T., Ma, X., Zhao, L., Du, Z., 2024. Automatic pine wilt disease detection based on improved YOLOv8 UAV multispectral imagery. Eco. Inform. 84, 102846. https://doi.org/10.1016/j.ecoinf.2024.102846.
Yasir, S.M., Ahn, H., 2022. Deep learning-based 3D instance and semantic segmentation: a review. Journal on Artificial Intelligence 4 (2), 99–114. https://doi.org/10.32604/jai.2022.031235.
Zhang, Y., Yang, W., Sun, Y., Chang, C., Yu, J., Zhang, W., 2021. Fusion of multispectral aerial imagery and vegetation indices for machine learning-based ground classification. Remote Sens. 13 (8). https://doi.org/10.3390/rs13081411.
Zhou, H., Wu, S., Xu, Z., Sun, H., 2024. Automatic detection of standing dead trees based on improved YOLOv7 from airborne remote sensing imagery. Front. Plant Sci. 15, 1278161. https://doi.org/10.3389/fpls.2024.1278161.